Extensional Flow of a Two-Dimensional Polymer Liquid Crystal

Pier Luca Maffettone and Massimiliano Grosso

Dipartimento di Ingegneria Chimica, Università Federico II Napoli, Piazzale Tecchio 80, I-80125 Napoli, Italy

Matthew C. Friedenberg and Gerald G. Fuller*

Department of Chemical Engineering, Stanford University, Stanford, California 94305-5025

Received March 8, 1996; Revised Manuscript Received August 20, 1996[⊗]

ABSTRACT: The transient behavior of a polymeric nematic liquid crystal interface in extensional flows is studied both experimentally and theoretically. Monolayers of the hairy rod polymer phthalocyaninatopolysiloxane subjected to two-dimensional, transient, extensional flows are modeled with the two-dimensional analogue of the rigid rod model. The scalar order parameter and the director orientation are compared with the experimental observables. Two parameters appear in the model: an average rotational diffusivity and the intensity of the nematic field. The average rotational diffusivity is determined by fitting relaxation experiments. The intensity of the nematic field, which is modeled with the Onsager potential, is determined by starting from the molecular parameters. A good quantitative agreement is obtained between experiments and theoretical predictions.

Introduction

The processing of polymer thin-film structures is of considerable interest to the performance of devices used in microelectronics and optoelectronics. Furthermore, order in two-dimensional systems is of general interest as model systems for understanding ordering in mesophases of smectic liquid crystals. Rigid, rodlike polymers are of particular interest in thin films due to their high stability, nonlinear optical properties, and use as alignment layers for liquid crystal displays. As in the case of three dimensions, when confined to two dimensions, high aspect ratio rigid polymers will experience steric interactions and undergo an isotropic−nematic transition. This phenomenon has been explored by Marrucci and Maffettone[1] using a rigid rod model originally suggested by Hess[2] and Doi[2] and restricted to two dimensions. This problem has also been recently taken up by Chen[4] using a worklike chain model with variable persistance length.

The fluid mechanical response of polymer liquid crystals in three dimensions is characterized by a highly nonlinear rheology that includes several phenomena that distinguish them from isotropic polymeric liquids. These incluce oscillatory shear stresses and optical anisotropies (birefringence and dichroism) during transient start up and flow reversal, transition from positive to negative first normal stress differences, and strain scaling of transient mechanical and optical responses.[5,6] The first model to explain these observations was the two-dimensional model of Marrucci and Maffettone. The restriction of the Doi model to two dimensions allowed for simpler calculations, but was still able to qualitatively predict much of the experimentally observed rheological behavior of three-dimensional systems. Since the first report on the two-dimensional version of the theory, however, Larson[7] has numerically solved the full three-dimensional case. The extension to three dimensions is able to offer new predictions, such as the behavior of the second normal stress differences, but many of the predictions of the three-dimensional model carry directly over to two dimensions.

Recently, optical measurements in our laboratory of monolayers of the hairy rod polymer phthalocyaninatopolysiloxane (PcPS) subject to two-dimensional extensional flow have yielded the first measurements of in situ flow-induced orientation of polymer chains at the air−water interface. These results, which are described in detail in ref 8, suggest that this system does form a two-dimensional liquid crystal and its anisotropic at rest. The purpose of the present paper is to explore the ability of the Marrucci−Maffettone model to quantitatively predict the observed fluid dynamical behavior. Furthermore, many aspects of the response of liquid crystalline materials to extensional flows are more easily explored in two dimensions. This is due to the fact that the high optical anisotropy and texture of liquid crystals normally make it necessary to use very thin flow geometries if techniques such as visual observation or flow birefringence are to be used to monitor flow-induced structure. However, the use of such flow cells leads to kinematics that are mixtures of simple shear and extensional flows. As was demonstrated in ref 8, this complication can be eliminated in two-dimensional samples.

Materials and Methods

The experiments determined orientation in a monolayer of PcPS chains using dichroism, $\Delta n''$. This optical property is linked to anisotropy in the imaginary part of the refractive index tensor. For PcPS polymer chains, this results from the strong optical absorption of the molecules in the green part of the spectrum. Since this absorption is strongly dependent on the relative orientation of the polarization of the light and the axis of the molecules, it can be used effectively to measure the orientation of the chains. Specifically, the dichroism is the difference in the eigenvalues of the imaginary part of the refractive index tensor, n''_{ij}, and is proportional to the scalar order parameter.

The monolayers were formed on a Langmuir trough, allowing the thermodynamic state of the film to be controlled. Flow in the monolayer was generated using a four-roll mill to induce a homogeneous, extensional flow as shown in Figure 1. This device imparts a flow characterized by hyperbolic streamlines by rotating the rollers. Reversal of the flow is easily accomplished by changing the direction of roller rotation, as shown. A stagnation point is located at the geometric center of the device and at this location there is no motion. This allows material to reside at this location for the greatest length

* Corresponding author.

[⊗] Abstract published in *Advance ACS Abstracts,* November 15, 1996.

S0024-9297(96)00359-2 CCC: $12.00

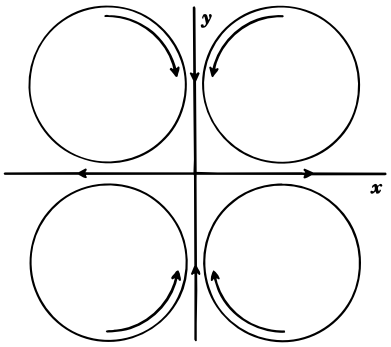

Figure 1. Schematic diagram of the four-roll mill. The direction of the rollers can be reversed to impart flow in the opposite direction.

of time. However, the velocity gradient is remarkably constant throughout the interior region of the rollers and the flow can be approximated as homogeneous. The optical measurements discussed below are all taken with the sampling volume in the vicinity of the stagnation point.

The monolayers were formed by spreading solutions of PcPS with different solvents on top of water. As pointed out earlier, PcPS is highly dichroic due to its strong absorption in the green part of the visible spectrum. This property was used to measure the flow-induced orientation of the monolayer in spite of the fact that the sample thickness is only that of a single molecular diameter. To accomplish these measurements, a polarization modulation scheme similar to that described in ref 9 was used. A "green" He−Ne laser was used to generate light at 543.6 nm. This was followed by a polarizer, photoelastic modulator, and a quarter wave plate. These elements were stationed above the Langmuir trough, and the light was directed through the stagnation point of the four-roll mill and normal to the liquid−air interface. Immersed in the subphase of the trough was a photodiode detector, which measured the transmitted light intensity. Analysis of the signal yielded the optical anisotropy $\delta'' = 2\pi\Delta n'' d/\lambda$, where d is the sample thickness and λ is the wavelength of the light. Also determined was the angle α that defines the average orientation of the PcPS rods relative to the horizontal axis of the mill.

The film-forming characteristics of PcPS have been studied in detail by Wegner and co-workers.[10] Although pure PcPS can be effectively spread on water, the result is a highly brittle and stiff film that does not readily deform under the action of flow. Instead, films of neat PcPS fracture in flow. Images of such films using Brewster angle microscopy reveal a response similar to "ice flow", with domains of molecules breaking up and producing a highly nonlocal fluid motion. For that reason, we have chosen to fluidize our samples by dissolving the PcPS within amphiphilic solvents such as arachidyl alcohol. Our sample of PcPS was obtained from Professor G. Wegner of the Max Planck Institute in Mainz, Germany, and had a degree of polymerization of approximately 100 but was quite polydisperse. This was blended at 5 mol % in arachidyl alcohol. These were spread on top of water and measurements were made at a temperature of 25 °C and compressed to a surface pressure of 20 mN/m. Flow visualization experiments made using particles of sulfur indicated that the surface was very close to ideal hyperbolic flow.

Upon compression of the film the surface pressure abruptly increases for this system once the area per repeat unit is decreased below 25 Å.[2] At this transition, the dichroism achieves a steady, time-dependent value once a continuous monolayer is established. Since the system is oriented at rest, a convenient experimental protocol is to subject the sample to a series of flow reversals. This procedure, which is also used in the study of bulk polymer liquid crystals, has the flow first generated in one direction for a period of time sufficient to induce a steady state and then reversed for the same amount of time. In this manner, the initial condition of the material can be conveniently established.

The Rigid Rod Model

The monolayer is formed of polymers that can be treated as rigid rods. All the molecules lie on a single plane. The model assumes that the sample is monodisperse; that is all the molecules are identical. No spatial inhomogeneity is accounted for. The orientation of a rod is determined by a unit vector $\mathbf{u} \equiv [\cos(\theta),\sin(\theta)]$, or equivalently by a single polar angle θ. This angle is measured with respect to an arbitrary direction (usually the flow direction). The orientational distribution function $\psi(t,\mathbf{u})$, or $\psi(t,\theta)$, gives the probability density that a rod is oriented along $\mathbf{u}$ at time t.

The Smoluchowski equation or diffusion equation for the distribution function as derived by Hess[2] and Doi[3] is:

$$\frac{\partial\psi}{\partial t} = \mathbf{D}\frac{\partial}{\partial\mathbf{u}}\cdot\left[\frac{\partial\psi}{\partial\mathbf{u}} + \frac{\psi}{k_B T}\frac{\partial\mathbf{V}(\mathbf{u})}{\partial\mathbf{u}}\right] - \frac{\partial}{\partial\mathbf{u}}\cdot(\dot{\mathbf{u}}\psi) \qquad (1)$$

In eq 1, $\partial/\partial\mathbf{u}$ is the gradient operator on the unit sphere, D is an average rotational diffusivity, $k_B T$ is the Boltzmann factor, $V(\mathbf{u})$ represents a mean field nematic potential, and $\dot{\mathbf{u}}$ is the rate of change of $\mathbf{u}$ due to the macroscopic flow. Equation 1 states that, in dynamic conditions, the orientational distribution function may change for three reasons: Brownian motion, excluded volume or other energetic interactions described by $V(\mathbf{u})$, and macroscopic flow. Equation 1 has been studied in its two-dimensional form by Marrucci and Maffettone[1,11] for the case of shear flows.

In this work, the nematic field is modeled following Onsager[12]:

$$V(\mathbf{u}) = Uk_B T\int\psi(\mathbf{u}')\sin(\mathbf{u}\mathbf{u}')\,d\mathbf{u}' \qquad (2)$$

In eq 2, U is the nondimensional intensity of the nematic field. In two dimensions U is equal to cl^2, where c is the number of rods per unit area and l is the rod length. The latter relation is obtained by neglecting terms of order d/l, where d is the rod diameter.

The rate of change of $\mathbf{u}$ depends on the velocity gradient $\mathbf{K}$:

$$\dot{\mathbf{u}} = \mathbf{K}\cdot\mathbf{u} - \mathbf{K}:\mathbf{uuu} \qquad (3)$$

and in the case of elongational flow considered here, $\boldsymbol{K}$ is

$$\mathbf{K} = \begin{vmatrix} \dot{\epsilon} & 0 \\ 0 & -\dot{\epsilon} \end{vmatrix} \qquad (4)$$

where $\dot{\epsilon}$ $(=\partial v_x/\partial x)$ is the strain rate. The geometry of the problem is taken so that $\theta = 0$ coincides with the x-coordinate.

The experimental results discussed below were conducted on a polymer monolayer and are in terms of two observable quantities: the dichroism and the average orientation of the sample. These quantities are related to information contained in the second moment of the orientational distribution function: the director orientation α, and the scalar order parameter S. The director is the unit vector defining the average sample orientation direction here measured with respect to $\theta = 0$; the scalar order parameter measures the spread around this average orientation and is proportional to the dichroism. These two quantities are easily calculated by introducing the second rank order tensor $\langle\mathbf{uu}\rangle$, i.e., the second moment of the distribution function:

$$\langle \mathbf{uu} \rangle(t) = \int \mathbf{uu}\, \psi(\mathbf{t},\mathbf{u})\, \mathrm{d}\mathbf{u} \tag{5}$$

where the integral is made over the configuration space, i.e., over the unit circle.

The scalar order parameter is

$$S = 2\lambda - 1 \tag{6}$$

where λ is the largest of the two eigenvalues of $\langle \mathbf{uu} \rangle$.

The director orientation angle is calculated as

$$\alpha = \arctan(\nu_2/\nu_1) \tag{7}$$

where ν_1 and ν_2 are the components of the eigenvector corresponding to λ.

Equation 1 has been numerically solved by expanding $\psi(t,\theta)$ in terms of a truncated Fourier series:

$$\psi(t,\theta) = \sum_{\substack{m=-n \\ m \text{ even}}}^{n} b_m(t) \mathrm{e}^{im\theta} \tag{8}$$

where the coefficients b_m are complex. Note that the m takes only even values for the periodicity of ψ. Since the distribution function is real, the following property holds true:

$$b_{-m} = (-1)^m b_m^* \tag{9}$$

where b_m^* represents the complex conjugate of b_m.

It should be remarked that the expansion fulfills the periodicity of the distribution function and of its derivatives, and the normalization of the distribution function determines the value of the coefficient b_0 ($=1/\pi$).

By applying a Galerkin procedure, the Smoluchowski equation is then reduced to a set of ordinary differential equations that can be written as

$$\frac{\mathrm{d}b_i}{\mathrm{d}t} = D\left[-i^2 b_i + 2U \sum_{\substack{m=-n \\ m \text{ even}}}^{n} \sum_{\substack{p=-n \\ p \text{ even}}}^{n} \delta_{i,m+p} \frac{b_m b_p (p^2 + pm)}{(p+1)(p-1)}\right] + \dot{\epsilon} \sum_{\substack{m=-n \\ m \text{ even}}}^{m=n} b_m[(0.5m+1)\delta_{i,m+2} - (0.5m-1)\delta_{i,m-2}] \tag{10}$$

where δ represents the Kronecker delta. The index i takes only even values from 2 to n. Note finally that eq 10 is still in dimensional form. It contains three parameters: D, U, and $\dot{\epsilon}$. Two of these parameters, D and U, have to be determined in order to compare the theoretical predictions with the experimental results. The strain rate $\dot{\epsilon}$ appearing in eq 10 is the independent experimental variable.

The scalar order parameter and the director orientation are easily calculated in terms of coefficients b_i:

$$S = \pi \bmod(b_2) \tag{11}$$

$$\alpha = \frac{1}{2} \arg(b_2)$$

The results presented in this work have been obtained truncating the expansion at $n = 40$, since for this value the accuracy of our simulations is adequate for $U < 15$ and $\dot{\epsilon} < 20\ \mathrm{s}^{-1}$. Most of the results here presented have been obtained by integrating the set of eqs 10 with Mathematica. Some results have been obtained by using a continuation software.[13]

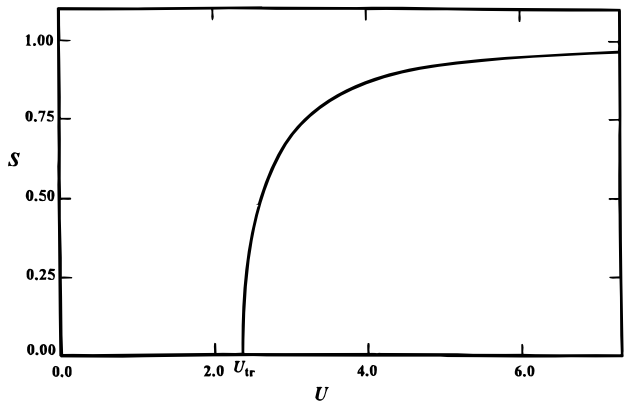

Figure 2. Model prediction in absence of flow. The scalar order parameter S is reported versus the nondimensional intensity of the nematic field U. At $U = U_{tr} \approx 2.35$ the transition from isotropic to nematic phase takes place.

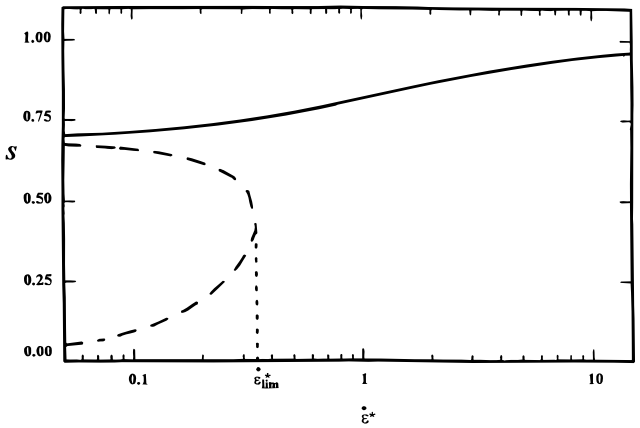

Figure 3. Scalar order parameter S versus the nondimensional strain rate $\dot{\epsilon}^*$ for $U = 3$. The solid line represents the stable stationary solution and the dashed line represents the unstable stationary solution. For $\dot{\epsilon}^* < \dot{\epsilon}^*_{\mathrm{lim}}$ three stationary solutions are predicted.

Model Predictions

The results presented in this section are in terms of a nondimensional time, $t^* = tD$, and nondimensional strain rate $\dot{\epsilon}^* = \dot{\epsilon}/D$.

First, it is useful to report the equilibrium behavior of the two-dimensional rigid-rod model with the Onsager potential. It is the equilibrium predictions that are used to fit the model with the experimental results. Figure 2 reports the scalar order parameter S versus the nondimensional intensity of the nematic field U. The isotropic−nematic transition takes place for $U_{tr} \approx 2.35$. For $U < U_{tr}$, only an isotropic stable solution ($S = 0$) is predicted at equilibrium, whereas for $U > U_{tr}$, a stable nematic solution and an unstable isotropic solution are found. As is well known, in two dimensions the isotropic−nematic phase transition is of second order.

Figure 3 reports the scalar order parameter versus the strain rate for steady-state conditions for $U = 3$ in a semilogarithmic plot. The solid line represents the stable stationary solution, whereas the dashed line represents unstable stationary solutions. It should be noted that for relatively large values of the strain rate the scalar order parameter increases slowly with the strain rate; i.e., a sort of saturation is predicted, in

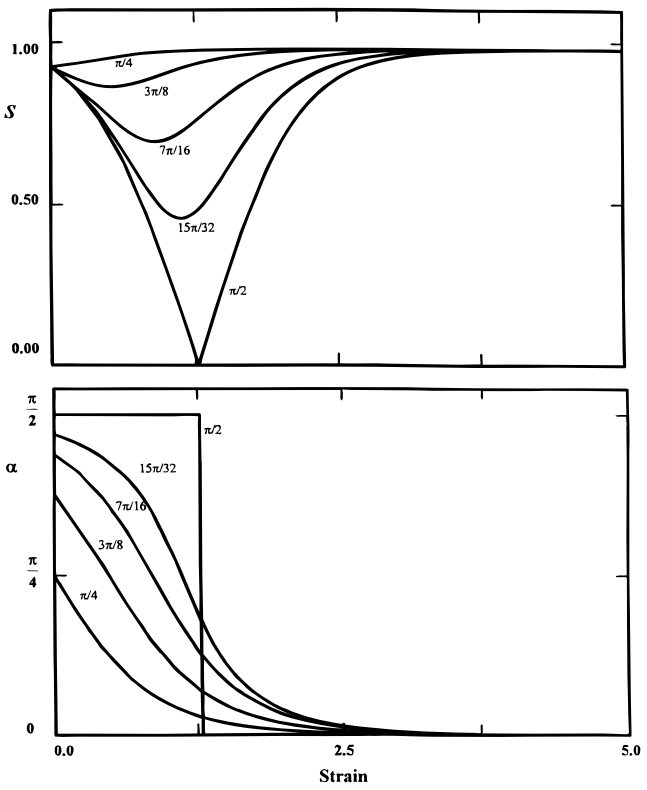

Figure 4. Transient response after start up from equilibrium for $U = 5$ and $\dot{\epsilon}^* = 20$ for a number of different initial orientations. In the upper plot, the scalar order parameter S is reported versus the strain. In the lower part, the director orientation α is plotted against the strain.

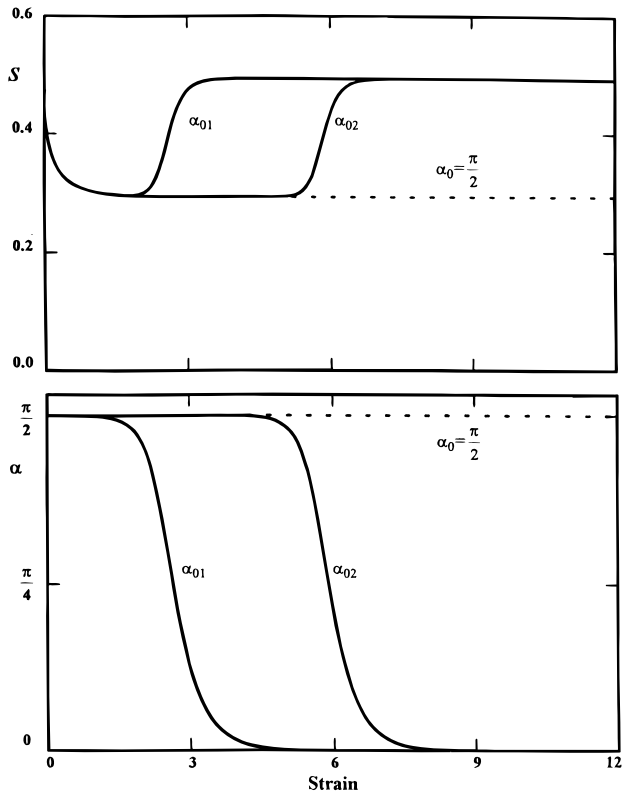

Figure 5. Transient response after start up from equilibrium for $U = 2.55$ and $\dot{\epsilon}^* = 0.057$ for two different initial orientations ($\alpha_{10} = (\pi/2)(1 - 10^{-4})$ and $\alpha_{20} = (\pi/2)(1 - 10^{-9})$). In the upper plot, the scalar order parameter S is reported versus the strain. In the lower part, the director orientation α is plotted against the strain. The dashed line represents the unstable solution which would be reached if the initial orientation is perfectly orthogonal to the flow direction.

agreement with the experimental results of ref 8. Needless to say, the director orientation at the steady state is that imposed by the flow conditions, $\alpha = 0$ or 90°, depending on the sign of $\dot{\epsilon}^*$. For $\dot{\epsilon}^* < \dot{\epsilon}^*_{\text{lim}}$ two unstable solutions are predicted. Both unstable solutions are oriented orthogonally with respect to the flow direction. These solutions have a scalar order parameter smaller than the equilibrium value and are obviously unstable because any perturbation of the director orientation induces an evolution toward the direction imposed by the flow through a rotation of the director. However, the unstable solutions could be of some importance as far as transient flows are concerned. It should be reported, finally, that the value of $\dot{\epsilon}^*_{\text{lim}}$ depends on U. We have determined via continuation the locus of $\dot{\epsilon}^*_{\text{lim}}$ as U is varied. For $U < 15$, the following interpolation was found:

$$\dot{\epsilon}^*_{\text{lim}} = \left(\frac{U - U_{\text{tr}}}{2.663}\right)^{1.446} \tag{12}$$

where U_{tr} is the value of U at the transition from isotropic to nematic conditions at equilibrium.

Transient results are presented in Figure 4 and in Figure 5. Figure 4 reports S and α as a function of strain for $U = 5$ and $\dot{\epsilon}^* = +20$. All the curves have been obtained starting from the equilibrium distribution oriented along different initial angles α_0. For $\alpha_0 < 45°$, the distribution function rotates toward the flow direction, and S steadily increases. Conversely, for $\alpha_0 > 45$, an initial decrease of the scalar order parameter is predicted. For $\alpha = 90°$, that is for an initial orientation orthogonal to the flow direction, the scalar order parameter first goes to zero and then increases to attain the stationary value. Correspondingly, the director orientation flips from 90° to 0° when S becomes nil. When the initial orientation is orthogonal to the flow direction, the flow cannot rotate the director due to the particular symmetry of the problem, whereas it is able to spread the distribution function, thus reducing the scalar order parameter. The system then becomes nearly isotropic, and subsequently the flow leads to a distribution function peaked around $\theta = 0°$. As a matter of fact, when S is close to zero the distribution function becomes quadrupolar, and this can again be explained by the specific symmetries of the hyperbolic flow.

If $\dot{\epsilon}^*$ is lower than a critical value ($\dot{\epsilon}^*_{\text{lim}}$ of Figure 3), the flow is weak with respect to the nematic potential, and a different situation arises. Figure 5 shows the transients for $U = 2.55$ $\dot{\epsilon}^* = 0.057$ (the different U value has been chosen for plotting clarity). Again the scalar order parameter and the director orientation are reported versus the strain. Two initial conditions are considered. The unstable stationary solution that would be reached if starting from $\alpha_0 = 90°$ is reported with the dashed line, the other two curves start from $\alpha_{10} = (\pi/2)(1 - 10^{-4})$ and $\alpha_{20} = (\pi/2)(1 - 10^{-9})$. When $\alpha_0 = 90°$, the distribution function reaches an unstable stationary solution which is eventually left in the presence of any infinitesimal perturbation. On the other hand, if α_0 is slightly different from 90°, the system initially spends some time close to the unstable solution, and eventually attains the stable stationary solution through a rotation of the director. The time spent close to the unstable solution depends on the initial condition: the closer the initial orientation angle is to 90°, the longer the system remains close to the

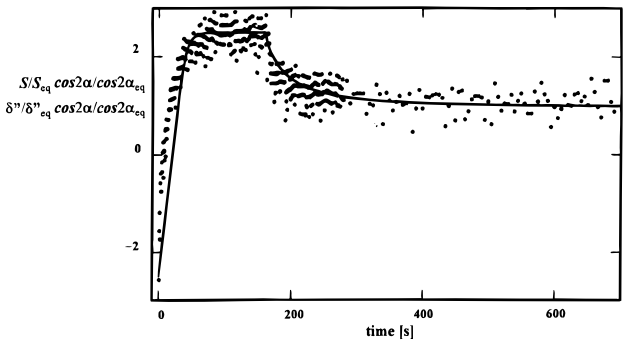

Figure 6. Comparison of the model prediction with the experimental results. The solid line represents $S \cos 2\alpha/(S_{eq} \cos 2\alpha_{eq})$ and the dots represent $\delta'' \cos 2\alpha/(\delta''_{eq} \cos 2\alpha_{eq})$ experimentally measured with 5 mol % PcPS in arachidyl alcohol. These quantities are reported versus the dimensional time. At $t = 0$ a flow reversal takes place, $\dot{\epsilon} = 0.04\ s^{-1}$. At $t \approx 180$ s the flow is stopped and a relaxation takes place. The predictions are obtained with $U = 2.45$ and $D = 2.749\ s^{-1}$.

unstable solution. This behavior is explained by considering Figure 3, which shows that for $\dot{\epsilon}^* < \dot{\epsilon}^*_{lim}$, two unstable stationary solutions are predicted. During the transient for $\dot{\epsilon}^* < \dot{\epsilon}^*_{lim}$ and with $\alpha_0 = 90°$, the state of the system remains at the unstable solution of Figure 3 with the higher scalar order parameter until a perturbation removes the system from the unstable solution. Now, in a flow reversal experiment such as the one presented in a previous section, after a first extensional flow the second extensional flow is oriented orthogonally to the first. The orientation attained after the first deformation is indeed almost orthogonal to the direction imposed by the subsequent flow. Thus, one should observe an evolution such as that reported in Figure 5 if $\dot{\epsilon}^* < \dot{\epsilon}^*_{lim}$.

Comparison with the Experiments

The agreement between the theoretical predictions and the experimental results can be assessed by comparing the optical anisotropy and the average orientation of the sample with the scalar order parameter and the director orientation. These quantities are normalized with respect to their equilibrium values, since in such a form they are directly comparable. Two parameters, the rotational diffusivity and the nondimensional intensity of the nematic field, must be determined to proceed with the comparison of the experimental results with the theoretical predictions.

First, the average rotational diffusivity is considered. Figure 6 reports the results of the flow reversal followed by flow cessation (compare Figure 13 of ref 8). In Figure 6, the dots, plotted versus the dimensional time, represent the quantity $\delta'' \cos 2\alpha/(\delta''_{eq} \cos 2\alpha_{eq})$ experimentally measured. The subscript eq refers to the conditions attained after the relaxation; needless to say, the angle α does not change during the relaxation. At time zero the flow is reversed, with $\dot{\epsilon} = 0.04\ s^{-1}$. The steady state is reached after about 160 s. At this time, the flow is stopped and relaxation takes place. The rotational diffusivity is here considered to be a constant, and its value is determined from the relaxation data of Figure 6. As noted by Friedenberg et al.,[8] the relaxation experiment can be well fitted with a single negative exponential. Thus, the diffusivity can be deduced from the experiments by nonlinearly fitting the optical

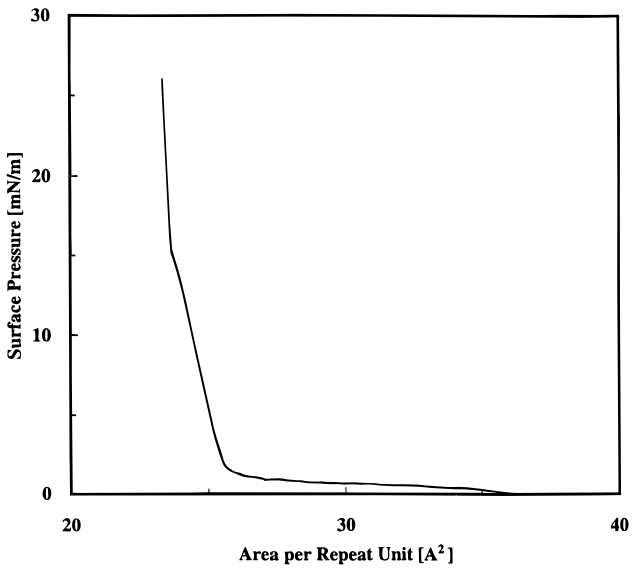

Figure 7. Pressure−area diagram for the PcPS solutions. The surface pressure is reported versus the area per repeat unit. The solution used in this work is the 5 mol % PcPS in arachidyl alcohol.

anisotropy relaxation transient (see Figure 6) with the model:

$$\delta'' = k_1 + k_2 e^{-Dt} \tag{13}$$

For the case of relaxation following the cessation of a flow strong enough to induce a saturation of orientation (the case represented in Figure 13 of ref 8), a good fit is obtained with $k_1 = 3.78 \times 10^{-5}$, $k_2 = 5.60 \times 10^{-5}$, and $D = 2.749 \times 10^{-2}\ s^{-1}$.

The U value can be derived by molecular parameters. As already mentioned, U for monodisperse sample is in fact equal to cl^2, where c is the number of rods per unit area and l represents the rod length. The concentration can be determined from Figure 7, where the pressure−area diagram for the solutions of PcPS is reported. All the experiments were conducted with a surface pressure of 30 mN/m, and thus the area per repeat unit was ca. 20. For the 5 mol % solution, the number of rods per unit area can be estimated as

$$c = \frac{1}{400\mathrm{DP}} \tag{14}$$

where DP represents the degree of polymerization which is ca. 100 for the PcPS used. Then, by considering that the monomer length is 3.4 Å, one finally obtains an estimate for the intensity of the nematic field:

$$U = \frac{3.4^2}{400}\mathrm{DP} \approx 2.9 \tag{15}$$

Actually, the U value chosen for the comparison has also been determined by the experiments. By noting that the scalar order parameter will be reduced by a certain amount during the relaxation (see Figure 6), the U value is the one which determines a change of the scalar order parameter by a factor of $(k_1 + k_2)/k_1$ ($\approx$2.48) when the stationary solution for $\dot{\epsilon} = 0.04\ s^{-1}$ relaxes to the equilibrium condition. For the experiment performed with a solution of PcPS in 5% of arachidyl alcohol, one determines $U \cong 2.45$ by using the equilibrium data reported in Figure 2. It is apparent that this value is very close to that determined starting from the Onsager

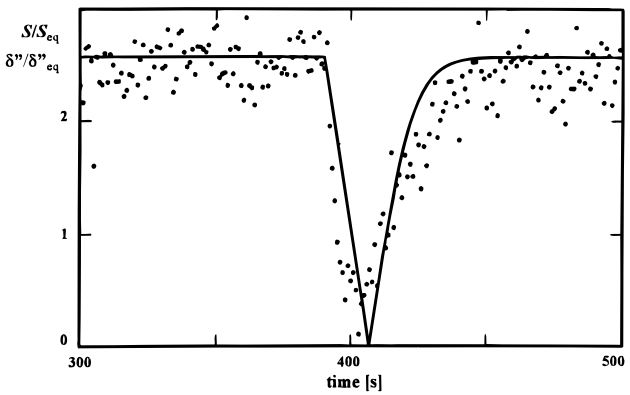

Figure 8. Comparison of the model prediction with the experimental results. The solid line represents S/S_{eq} and the dots represent δ''/δ''_{eq} experimentally measured with 5 mol % PcPS in arachidyl alcohol. These quantities are reported versus the dimensional time. At $t \approx 390$ s the flow is reversed, $\dot{\epsilon} = 0.05\ s^{-1}$. The predictions are obtained with $U = 2.45$ and $D = 2.749\ s^{-1}$.

approach. All the parameters needed to compare the predictions with the experiments are then determined.

In Figure 6, the quantities $S \cos 2\alpha/(S_{eq} \cos 2\alpha_{eq})$, determined with $D = 2.749 \times 10^{-2}\ s^{-1}$ and $U = 2.45$, are represented with a solid line. The agreement between the theoretical predictions and the experimental results is very good. The model prediction falls in between the scattered experimental data, at the steady state as well as during the relaxation process. A discrepancy exists during the transient following the flow inversion, where the experimental data are all above the theoretical curve.

Figure 8 shows the comparison of an independent flow reversal transient experiment (Figure 9 of ref 8). The ratios S/S_{eq} (solid line) and δ''/δ''_{eq} (dots) are reported versus the dimensional time. Again the agreement is very good: the stationary values and the time constants are correctly predicted by the model. Furthermore, the time at which the scalar order parameter and the dichroism attain their minimum value nearly coincide.

The observed slight discrepancy may be attributed to many factors not accounted for in the modeling. In fact, the system has been considered as a homogeneous and monodisperse bulk of perfectly rigid rods. The rotational diffusivity has been considered constant. In this regard, however, no apparent improvement of the results is obtained when a rotational diffusivity which depends on the scalar order parameter is considered.

Conclusions

The comparison between the model predictions and the experiments indicates that the two-dimensional polymer liquid crystal model is able to capture many of the essential features of the data. The strength of the nematic potential is determined from molecular parameters, and through adjustment of rotational diffusivity, the model is able to produce adequate, quantitative fits to two separate transient experiments in extensional flow. The success of the simulation of the data suggests that it should be possible to use this procedure to acquire data on the rotational diffusivity of anisotropic polymers in two dimensions. Furthermore, by obtaining data on the strength of the nematic potential as a function of polymer concentration, it should be feasible to directly determine the form of the potential function itself. Experiments are presently underway where the concentration will be systematically varied so that the scaling of these two physical properties with concentration can be resolved.

This work also suggests that qualitative differences in the orientational dynamics should be observed for weak flows where $\dot{\epsilon}^* < \dot{\epsilon}^*_{lim}$. Presently, the only available data are in the strong-flow regime and future experiments are planned in both the strong- and weak-flow limits. Finally, one would expect qualitatively different dynamics to occur in simple shear flows where a rotational component is present. In such a flow, the model predicts director tumbling to occur where the orientation of the nematic will oscillate in time following transient flow transitions such as flow reversals. A parallel band apparatus capable of generating such a flow is presently available, and it is anticipated that results in simple shear will be available in the near future.

Acknowledgment. This work has been partly funded by MURST (60%) and by Programma Scambi Internazionali, University of Naples Federico II. Partial support was also received from the NSF Materials Research Science Engineering Center on Polymer Interfaces and Macromolecular Assemblies.

References and Notes

(1) Marrucci, G.; Maffettone, P. L. Description of the liquid crystalline phase of rodlike polymers at high shear rates. *Macromolecules* **1989**, *22*, 4076.
(2) Hess, S. Z. Fokker−Planck-Equation approach to flow alignment in liquid crystals. *Z. Naturforsch.* **1976**, *31A*, 1034.
(3) Doi, M. Molecular dynamics and rheological properties of concentrated solutions of rodlike polymers in isotropic and liquid crystalline phases. *J. Polym. Sci., Polym. Phys. Ed.* **1981**, *19*, 229.
(4) Chen, Z. Y. Continuous isotropic−nematic transition of partially flexible polymers in two dimensions. *Phys. Rev. Lett.* **1993**, *71*, 93.
(5) Moldenaers, P.; Fuller, G. G.; Mewis, J. Mechanical and optical rheometry of polymer liquid domain structure. *Macromolecules* **1989**, *22*, 960.
(6) Maffettone, P. L.; Marrucci, G.; Mortier, M.; Moldenaers, P.; Mewis, J. Dynamic characterization of liquid crystalline polymers under flow-aligning high-shear-rate conditions. *J. Chem. Phys.* **1994**, *100*, 7736.
(7) Larson, R. G. Arrested tumbling in shearing flows of liquid crystal polymers. *Macromolecules* **1990**, *23*, 3983.
(8) Friedenberg, M. C.; Fuller, G. G.; Frank, C. W.; Robertson, C. R. *In situ* optical studies of flow-induced orientation in a polymer monolayer. *Macromolecules* **1996**, *29*, 705.
(9) Fuller, G. G. *Optical Rheometry of Complex Fluids*; Oxford University Press: New York, 1995.
(10) Schwiegk, S.; Vahlenkamp, T.; Xu, Y.; Wegner, G. Origin of orientation phenomena in layered Langmuir−Blodgett structures of hairy-rod polymers. *Macromolecules* **1992**, *25*, 2513.
(11) Marrucci, G.; Maffettone, P. L. Nematic phase of rodlike polymers. I. Prediction of transient behavior at high shear rate. *J. Rheol.* **1990**, *34*, 1217.
(12) Onsager, L. The effect of shape on the interaction of colloidal particles. *Ann. N.Y. Acad. Sci.* **1949**, *51*, 627.
(13) Doedel, E. J.; Kernevez, J. P. AUTO: Software for Continuation and Bifurcation Problems in Ordinary Differential Equations, California Institute of Technology, 1986.

MA9603591